

# Generating entanglement between microwave photons and qubits in multiple cavities coupled by a superconducting qutrit

Chui-Ping Yang,<sup>1,2</sup> Qi-Ping Su,<sup>1</sup> Shi-Biao Zheng,<sup>3</sup> and Siyuan Han<sup>4</sup><sup>1</sup>*Department of Physics, Hangzhou Normal University, Hangzhou, Zhejiang 310036, China*<sup>2</sup>*State Key Laboratory of Precision Spectroscopy, Department of Physics, East China Normal University, Shanghai 200062, China*<sup>3</sup>*Department of Physics, Fuzhou University, Fuzhou 350002, China*<sup>4</sup>*Department of Physics and Astronomy, University of Kansas, Lawrence, Kansas 66045, USA*

(Received 20 December 2012; published 15 February 2013)

We discuss how to generate entangled coherent states of four microwave resonators (a.k.a. cavities) coupled by a three-level superconducting device (qutrit). We also show that a Greenberger-Horne-Zeilinger (GHZ) state of four superconducting qubits embedded in four different resonators can be created with this scheme. In principle, the proposed method can be extended to create an entangled coherent state of  $n$  resonators and to prepare a (GHZ) state of  $n$  qubits distributed over  $n$  cavities in a quantum network. In addition, it is noted that four resonators coupled by a coupler qutrit may be used as a basic circuit block to build a two-dimensional quantum network, which is useful for scalable quantum information processing.

DOI: [10.1103/PhysRevA.87.022320](https://doi.org/10.1103/PhysRevA.87.022320)

PACS number(s): 03.67.Bg, 03.67.Lx, 42.50.Dv, 85.25.Cp

## I. INTRODUCTION

Recent progress in circuit cavity QED, in which superconducting qubits play the role of atoms in atom cavity QED, makes it a standout among the most promising candidates for implementing quantum information processing (QIP) [1]. Superconducting qubits, such as charge, flux, and phase qubits, and microwave resonators (a.k.a. cavities) can be fabricated using modern integrated circuit technology, their properties can be characterized and adjusted *in situ*, they have relatively long decoherence times [2], and various single and multiple qubits operations with state readout have been demonstrated [3–7]. In particular, it has been demonstrated that a superconducting resonator provides a quantized cavity field which can mediate long-range and fast interaction between distant superconducting qubits [8–10]. Theoretically, it was predicted earlier that the strong-coupling limit can readily be realized with superconducting charge qubits [11] or flux qubits [12]. Moreover, the strong-coupling limit between the cavity field and superconducting qubits has been experimentally demonstrated [13,14]. All of these theoretical and experimental progresses make circuit cavity QED very attractive for QIP.

During the past decade, many theoretical proposals have been presented for the preparation of Fock states, coherent states, squeezed states, the Schrödinger cat state, and an arbitrary superposition of Fock states of a single superconducting resonator [15–18]. Also, experimental creation of a Fock state and a superposition of Fock states of a single superconducting resonator using a superconducting qubit has been reported [19,20]. On the other hand, a large number of theoretical proposals have been presented for implementing quantum information transfer, quantum logical gates, and quantum entanglement with two or more superconducting qubits placed in a cavity or coupled by a resonator (usually in the form of coplanar transmission line) [8,11,12,21–27]. Moreover, experimental demonstration of quantum information transfer, two-qubit gates, and three-qubit gates, as well as experimental preparation of three-qubit entanglement, have been reported with superconducting qubits in a cavity [9,28–31]. However, realistic

QIP will most likely need a large number of qubits and placing all of them in a single cavity quickly runs into many fundamental and practical problems such as the increase of cavity decay rate and decrease of qubit-cavity coupling strength.

Therefore, future QIP most likely will require quantum networks consisting of a large number of cavities, each hosting and coupled to multiple qubits. In this type of architecture, transfer and exchange of quantum information will not only occur among qubits in the same cavity, but also between different cavities. Hence, attention must be paid to the preparation of quantum states of two or more superconducting resonators (hereafter we use the term cavity and resonator interchangeably), preparation of quantum states of superconducting qubits located in different cavities, and implementation of quantum logic gates on superconducting qubits distributed over different resonators in a network. All of these ingredients are essential to realizing large-scale quantum information processing based on circuit QED. Recently, a theoretical proposal for the manipulation and generation of nonclassical microwave field states as well as the creation of controlled multipartite entanglement with two resonators coupled by a superconducting qubit has been presented [32], and a theoretical method for synthesizing an arbitrary quantum state of two superconducting resonators using a tunable superconducting qubit has been proposed [33]. Moreover, experimental demonstration of creating  $N$ -photon NOON states (entangled states  $|N0\rangle + |0N\rangle$ ) in two superconducting microwave resonators by using a superconducting phase qutrit coupled to two resonators [34] and shuffling one- and two-photon Fock states between three resonators interconnected by two superconducting phase qubits have been reported recently [35]. These works opened a new avenue for building one-dimensional linear quantum networks of resonators and qubits.

On the other hand, entanglement between the atomic states and the coherent states of a single-mode cavity was earlier demonstrated in experiments [36]. However, how to create entangled coherent states between two or more resonators, based on cavity QED, has not been reported.

As is well known, entangled coherent states are important in quantum information processing and communication. For instance, they can be used to construct quantum gates [37] (using coherent states as the logical qubits [38]), perform teleportation [39], build quantum repeaters [40], implement quantum key distribution [41], and entangle distant atoms in a network [42,43]. Moreover, it was first shown [44] that entangled coherent states can be used to test violation of Bell inequalities.

In this paper, we propose a way for generating entangled coherent states of four resonators using one three-level superconducting device (qutrit) as the intercavity coupler. This proposal operates essentially by bringing the transition between the two higher-energy levels of the coupler qutrit dispersively coupled to the resonator modes. In addition, we will show how to create a Greenberger-Horne-Zeilinger (GHZ) state of four superconducting qubits located in four different resonators using the coupler qutrit. The GHZ states are multiqubit entangled states of the form  $|00\dots 0\rangle \pm |11\dots 1\rangle$ , which are useful in quantum information processing [45] and communication [46].

Our proposal has the following advantages: (i) Only one superconducting qutrit is needed. (ii) The operation procedure and the operation time are both independent of the number of resonators as well as the number of qubits in the cavities. (iii) No adjustment of the resonator mode frequencies is required during the entire operation. (iv) The proposed method can in principle be applied to create entangled coherent states of  $n$  resonators and to prepare a GHZ state of  $n$  qubits distributed over  $n$  cavities in a quantum network, for which the operational steps and the operation time do not increase as  $n$  becomes larger.

This proposal is quite general, which can be applied to the case when the coupler qutrit is a different physical system with three levels, such as a quantum dot or a nitrogen-vacancy (NV) center. This work is of interest because it provides a way to generate entangled coherent states of multiple cavities and create a GHZ entangled state of qubits distributed over multiple cavities, which are important in quantum information processing and quantum communication. Finally, it is interesting to note that the four resonators coupled by a coupler qutrit can be used as a basic circuit block to build a two-dimensional quantum network, which may be useful for scalable quantum information processing.

This paper is organized as follows. In Sec. II, we review some basic theories of a coupler qutrit interacting with four or three resonators. In Sec. III, we discuss how to create four-resonator entangled coherent states. In Sec. IV, we show a way to generate a GHZ entangled state of qubits embedded in four cavities without measurement. In Sec. V, we give a discussion on the possibility of using the four resonators coupled by a coupler qutrit to build a two-dimensional quantum network. In Sec. III–V, we give brief discussions on the experimental issues and possible experimental implementation. A concluding summary is given in Sec. VI.

## II. BASIC THEORY

Consider a superconducting qutrit  $A$ , with states  $|0\rangle$ ,  $|1\rangle$ , and  $|2\rangle$ , coupled to four resonators 1, 2, 3, and 4 as shown in

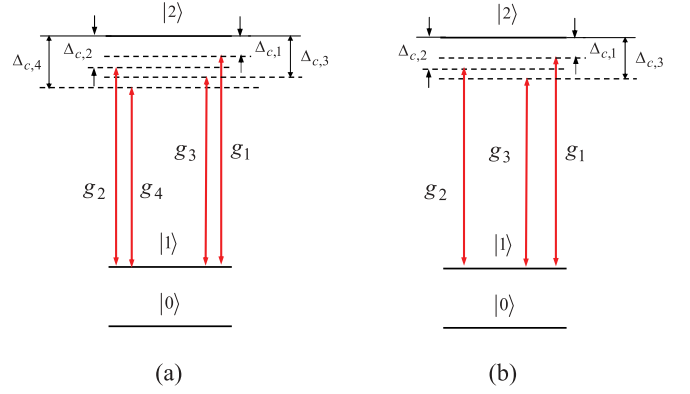


FIG. 1. (Color online) (a) Illustration of four resonators each dispersively coupled with the  $|1\rangle \leftrightarrow |2\rangle$  transition of qutrit  $A$ . Here,  $\Delta_{c,i}$  is the large detuning between the  $|1\rangle \leftrightarrow |2\rangle$  transition frequency of qutrit  $A$  and the frequency  $\omega_{c,i}$  of resonator  $i$ , which satisfies  $\Delta_{c,i} \gg g_i$  ( $i = 1, 2, 3, 4$ ). (b) Illustration of three resonators each dispersively coupled with the  $|1\rangle \leftrightarrow |2\rangle$  transition of qutrit  $A$ , with  $\Delta_{c,i} \gg g_i$  ( $i = 1, 2, 3$ ). For simplicity, we here consider the case that the  $|0\rangle \leftrightarrow |1\rangle$  level spacing is smaller than the  $|1\rangle \leftrightarrow |2\rangle$  level spacing. This type of level structure is available in superconducting charge qutrits or flux qutrits [27]. Alternatively, the  $|0\rangle \leftrightarrow |1\rangle$  level spacing can be larger than the  $|1\rangle \leftrightarrow |2\rangle$  level spacing, which applies to superconducting phase qutrits [27].

Fig. 1(a) or three resonators 1, 2, and 3 as depicted in Fig. 1(b). Suppose that the relevant mode frequency of each resonator is coupled to the  $|1\rangle \leftrightarrow |2\rangle$  transition while decoupled from transitions between other levels of the qutrit (Fig. 1). The Hamiltonian for the whole system is given by (assuming  $\hbar = 1$  for simplicity)

$$H = \sum_{i=1}^m \omega_{c,i} a_i^\dagger a_i + \frac{\omega_0}{2} S_z + \sum_{i=1}^m g_i (a_i S_+ + a_i^\dagger S_-), \quad (1)$$

where  $m = 4$  (3) corresponds to qutrit  $A$  coupled to four (three) resonators;  $S_+ = |2\rangle\langle 1|$ ,  $S_- = |1\rangle\langle 2|$ ,  $S_z = |2\rangle\langle 2| - |1\rangle\langle 1|$ ;  $a_i$  ( $a_i^\dagger$ ) is the photon annihilation (creation) operator of resonator  $i$  with frequency  $\omega_{c,i}$ ;  $\omega_0$  is the transition frequency between the two levels  $|1\rangle$  and  $|2\rangle$  of qutrit  $A$ ; and  $g_i$  is the coupling constant between the resonator  $i$  and the  $|1\rangle \leftrightarrow |2\rangle$  transition of qutrit  $A$ . In the interaction picture, the Hamiltonian (1) becomes

$$H_I = \sum_{i=1}^m g_i (e^{i\Delta_{c,i}t} a_i S_+ + e^{-i\Delta_{c,i}t} a_i^\dagger S_-), \quad (2)$$

where  $\Delta_{c,i} = \omega_0 - \omega_{c,i}$  is the detuning between the  $|1\rangle \leftrightarrow |2\rangle$  transition frequency  $\omega_0$  of qutrit  $A$  and the  $i$ th resonator frequency  $\omega_{c,i}$ . Suppose that (i) the  $|1\rangle \leftrightarrow |2\rangle$  transition of qutrit  $A$  is dispersively coupled to the resonator  $i$  (i.e.,  $\Delta_{c,i} \gg g_i$ ) (Fig. 1); and (ii)  $\Delta_{c,i+1} - \Delta_{c,i}$  is on the same order of magnitude as the coupling constant  $g_i$ , such that the indirect interaction between any two resonators induced by qutrit  $A$  is negligible. Under these conditions, the Hamiltonian (2) reduces to [47]

$$H_{\text{eff}} = \sum_{i=1}^m \frac{g_i^2}{\Delta_{c,i}} (a_i a_i^\dagger |2\rangle\langle 2| - a_i^\dagger a_i |1\rangle\langle 1|). \quad (3)$$

One can see that the Stark shift terms  $\sum_{i=1}^m g_i^2 a_i a_i^\dagger |2\rangle \langle 2| / \Delta_{c,i}$  involved in the Hamiltonian (2) do not affect the state  $|1\rangle$  of qutrit  $A$  during the evolution.

Based on the Hamiltonian (3), it is easy to see that if the resonator  $i$  is initially in a coherent state  $|\alpha_i\rangle$ , the time evolution of the state  $|1\rangle_A |\alpha_i\rangle$  of the system composed of qutrit  $A$  and the resonator  $i$  is then described by

$$|1\rangle_A |\alpha_i\rangle \rightarrow |1\rangle_A |\alpha_i \exp(i g_i^2 t / \Delta_{c,i})\rangle, \quad (4)$$

which leads to the coherent state of the  $i$ th cavity evolving from  $|\alpha_i\rangle$  to  $|\alpha_i \exp(i g_i^2 t / \Delta_{c,i})\rangle$  when  $g_i^2 t / \Delta_{c,i} = \pi$ . The state  $|0\rangle_A |\alpha_i\rangle$  does not change under the Hamiltonian (3). The result (4) presented here will be employed for creating four-resonator entangled coherent states as discussed in the next section.

In addition, based on the Hamiltonian (3), it is easy to find that if the resonator  $i$  is initially in a single-photon state  $|1\rangle_{c,i}$ , the time evolution of the state  $|1\rangle_A |1\rangle_{c,i}$  of the system is then given by

$$|1\rangle_A |1\rangle_{c,i} \rightarrow e^{i g_i^2 t / \Delta_{c,i}} |1\rangle_A |1\rangle_{c,i}, \quad (5)$$

which introduces a phase flip to the state  $|1\rangle_A |1\rangle_{c,i}$  when the evolution time  $t$  satisfies  $g_i^2 t / \Delta_{c,i} = \pi$ . Note that the states  $|0\rangle_A |0\rangle_{c,i}$ ,  $|1\rangle_A |0\rangle_{c,i}$ , and  $|0\rangle_A |1\rangle_{c,i}$  remain unchanged under the Hamiltonian (3). This result (5) will be employed for generating a GHZ state of four qubits distributed over four different cavities.

It should be mentioned here that during the following entanglement preparation, the level  $|0\rangle$  of the coupler qutrit  $A$  is not affected by the mode of each resonator. To meet this condition, one can choose qutrit  $A$  for which the transition between the two lowest levels  $|0\rangle$  and  $|1\rangle$  is forbidden due to the optical selection rules [48], weak via increasing the potential barrier between the two lowest levels [2,49–51], or highly detuned (decoupled) from the cavity mode of each resonator, which can be achieved by adjusting the level spacings of qutrit  $A$ . Note that for superconducting devices, the level spacings can be readily adjusted by varying external control parameters [2,50,52].

### III. CREATION OF FOUR-RESONATOR ENTANGLED COHERENT STATES

In this section, we will show how to generate an entangled coherent state of four resonators, give a discussion of the fidelity of the operations, and then address issues which are relevant to this topic.

#### A. Generation of four-resonator entangled coherent states

Consider a system composed of four resonators and a superconducting qutrit  $A$  [Fig. 2(a)]. The qutrit  $A$  has three levels shown in Fig. 1. Initially, the qutrit  $A$  is decoupled from all resonators [Fig. 3(a)], which can be realized by a prior adjustment of its level spacings [2,50,52]. The qutrit  $A$  is initially prepared in the state  $(|0\rangle_A + |1\rangle_A) / \sqrt{2}$  and each resonator is initially prepared in a coherent state [16,20], i.e.,  $|\alpha_i\rangle$  for resonator  $i$  ( $i = 1, 2, 3, 4$ ). To prepare the four resonators in an entangled coherent state, we now perform the

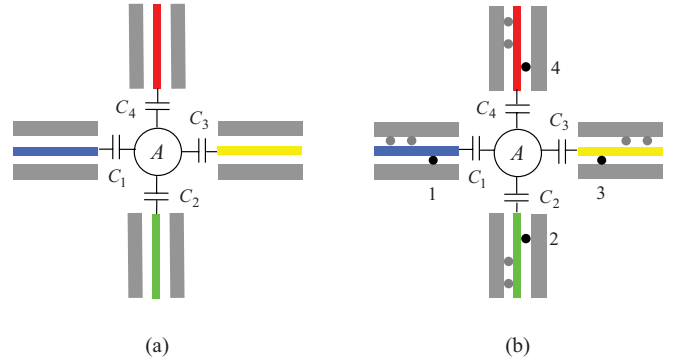


FIG. 2. (Color online) (a), (b) Diagram of a superconducting qutrit  $A$  (a circle at the center) coupled capacitively to four one-dimensional coplanar waveguide resonators through  $C_1, C_2, C_3, C_4$ , respectively. In (b), a black or gray dot in each resonator represents a qubit. The four black-dot qubits (1,2,3,4) are first prepared in a GHZ state, which can further be entangled with all other qubits (gray dots). For clarity, only three qubits in each cavity are shown.

following operations:

(i) Adjust the level spacings of the qutrit  $A$  such that the field mode for each resonator is dispersively coupled to the  $|1\rangle \leftrightarrow |2\rangle$  transition (i.e.,  $\Delta_{c,i} = \omega_{21} - \omega_{c,i} \gg g_i$  for resonator  $i$ ) while far off resonant with (decoupled from) the transition between other levels of the qutrit  $A$  [Fig. 3(b)]. After an interaction time  $\tau$ , the initial state  $(|0\rangle_A + |1\rangle_A) \prod_{i=1}^4 |\alpha_i\rangle$  of the whole system changes to (here and below a normalization

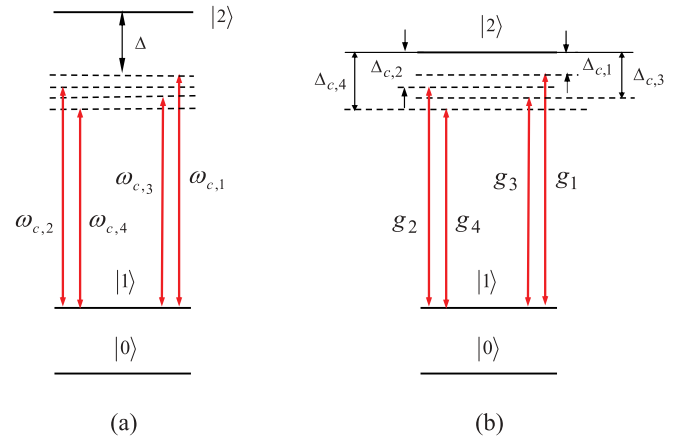


FIG. 3. (Color online) (a) Illustration of qutrit  $A$  decoupled from four cavities or resonators. Here,  $\Delta$  is the large detuning between the  $|1\rangle \leftrightarrow |2\rangle$  transition frequency of qutrit  $A$  and the frequency  $\omega_{c,1}$  of resonator 1, which represents that the  $|1\rangle \leftrightarrow |2\rangle$  transition of qutrit  $A$  is far off resonant with (decoupled from) resonator 1. Since the frequencies  $\omega_{c,1}, \omega_{c,2}, \omega_{c,3}$ , and  $\omega_{c,4}$  of four resonators 1, 2, 3, and 4 satisfy  $\omega_{c,1} > \omega_{c,2} > \omega_{c,3} > \omega_{c,4}$ , the  $|1\rangle \leftrightarrow |2\rangle$  transition of qutrit  $A$  is also far off resonant with (decoupled from) the other three resonators 2, 3, and 4. (b) Illustration of four resonators each dispersively coupled with the  $|1\rangle \leftrightarrow |2\rangle$  transition of qutrit  $A$ . Here,  $\Delta_{c,i}$  is the large detuning between the  $|1\rangle \leftrightarrow |2\rangle$  transition frequency of qutrit  $A$  and the frequency  $\omega_{c,i}$  of resonator  $i$ , which satisfies  $\Delta_{c,i} \gg g_i$  ( $i = 1, 2, 3, 4$ ).

factor is omitted for simplicity)

$$|0\rangle_A \prod_{i=1}^4 |\alpha_i\rangle + |1\rangle_A \prod_{i=1}^4 |\alpha_i \exp(i g_i^2 t / \Delta_{c,i})\rangle. \quad (6)$$

Both of the resonators and qutrit can be fabricated to have appropriate resonator frequencies and qutrit-cavity coupling strengths, such that  $\frac{g_1^2}{\Delta_{c,1}} = \frac{g_2^2}{\Delta_{c,2}} = \frac{g_3^2}{\Delta_{c,3}} = \frac{g_4^2}{\Delta_{c,4}}$ . Note that tunable coupling strength between a superconducting device and a cavity has been proposed and demonstrated experimentally [53–55]. For  $g_i^2 \tau / \Delta_{c,i} = \pi$  ( $i = 1, 2, 3, 4$ ), the system then evolves to

$$|0\rangle_A \prod_{i=1}^4 |\alpha_i\rangle + |1\rangle_A \prod_{i=1}^4 |-\alpha_i\rangle, \quad (7)$$

according to Eq. (6). Here,  $\langle \alpha_i | -\alpha_i \rangle = \exp(-2|\alpha_i|^2) \approx 0$  when  $\alpha_i$  is large enough.

(ii) Adjust the level spacings of the qutrit  $A$  to the original configuration such that it is decoupled (i.e., far off resonance) from all resonators [Fig. 3(a)]. We then apply a classical  $\pi/2$  pulse (resonant with the  $|0\rangle \leftrightarrow |1\rangle$  transition of the qutrit  $A$ ) to transform the qutrit state  $|0\rangle_A$  to  $|0\rangle_A + |1\rangle_A$  and  $|1\rangle_A$  to  $-|0\rangle_A + |1\rangle_A$ . Thus, the state (7) becomes

$$|0\rangle_A \left( \prod_{i=1}^4 |\alpha_i\rangle - \prod_{i=1}^4 |-\alpha_i\rangle \right) + |1\rangle_A \left( \prod_{i=1}^4 |\alpha_i\rangle + \prod_{i=1}^4 |-\alpha_i\rangle \right). \quad (8)$$

We now perform a measurement on the states of the qutrit  $A$  in the  $\{|0\rangle, |1\rangle\}$  basis. If the qutrit  $A$  is found in the state  $|0\rangle$ , it can be seen from Eq. (8) that the four resonators must be in the following entangled coherent state:

$$\mathcal{N}_- (|\alpha_1\rangle |\alpha_2\rangle |\alpha_3\rangle |\alpha_4\rangle - |-\alpha_1\rangle |-\alpha_2\rangle |-\alpha_3\rangle |-\alpha_4\rangle). \quad (9)$$

Similarly, if the qutrit is found in the state  $|1\rangle$ , then the four resonators must be in the following entangled coherent state:

$$\mathcal{N}_+ (|\alpha_1\rangle |\alpha_2\rangle |\alpha_3\rangle |\alpha_4\rangle + |-\alpha_1\rangle |-\alpha_2\rangle |-\alpha_3\rangle |-\alpha_4\rangle), \quad (10)$$

where  $\mathcal{N}_\mp$  are the normalization factors.

We should point out that since the level spacing between the two levels  $|1\rangle$  and  $|2\rangle$  of qutrit  $A$  in Fig. 3(a) is set to be greater than that in Fig. 3(b), qutrit  $A$  remains off resonant with any of the four resonators during tuning the level structure of qutrit  $A$  from Figs. 3(a) to 3(b).

It is straightforward to show that by using a superconducting qutrit coupled to  $n$  resonators ( $1, 2, \dots, n$ ) initially in the state  $\prod_{i=1}^n |\alpha_i\rangle$ , the  $n$ -resonator entangled coherent state  $\prod_{i=1}^n |\alpha_i\rangle - \prod_{i=1}^n |-\alpha_i\rangle$  or  $\prod_{i=1}^n |\alpha_i\rangle + \prod_{i=1}^n |-\alpha_i\rangle$  can be prepared by using the same procedure given above.

## B. Fidelity

Let us now give a discussion of the fidelity of the operations. Since only the qutrit-pulse resonant interaction is used in step (ii), this step can be completed within a very short time (e.g., by increasing the pulse Rabi frequency), such that the dissipation of the qutrit and the cavities is negligibly small. In this case, the dissipation of the system would appear in the operation of step (i) because of the qutrit-cavity dispersive interaction. During the operation of step (i), the dynamics of the lossy

system is determined by

$$\begin{aligned} \frac{d\rho}{dt} = & -i[H_I, \rho] + \sum_{i=1}^4 \kappa_i \mathcal{L}[a_i] + \{\gamma_\phi (S_z \rho S_z - \rho) + \gamma \mathcal{L}[S_-]\} \\ & + \{\gamma'_\phi (S'_z \rho S'_z - \rho) + \gamma' \mathcal{L}[S'_-]\} + \{\gamma''_\phi (S''_z \rho S''_z - \rho) \\ & + \gamma'' \mathcal{L}[S''_-]\}, \end{aligned} \quad (11)$$

where  $H_I$  is the Hamiltonian (2),  $\mathcal{L}[a_i] = a_i \rho a_i^\dagger - a_i^\dagger a_i \rho / 2 - \rho a_i^\dagger a_i / 2$ ,  $\mathcal{L}[S_-] = S_- \rho S_+ - S_+ S_- \rho / 2 - \rho S_+ S_- / 2$ ,  $\mathcal{L}[S'_-] = S'_- \rho S'_+ - S'_+ S'_- \rho / 2 - \rho S'_+ S'_- / 2$ , and  $\mathcal{L}[S''_-] = S''_- \rho S''_+ - S''_+ S''_- \rho / 2 - \rho S''_+ S''_- / 2$  (with  $S'_z = |2\rangle \langle 2| - |0\rangle \langle 0|$ ,  $S''_z = |1\rangle \langle 1| - |0\rangle \langle 0|$ ,  $S'_- = |0\rangle \langle 2|$ , and  $S''_- = |0\rangle \langle 1|$ ). In addition,  $\kappa_i$  is the photon decay rate of the cavity  $i$ ,  $\gamma_\phi$  and  $\gamma$  are the dephasing rate and the energy relaxation rate of the level  $|2\rangle$  of qutrit  $A$  for the decay path  $|2\rangle \rightarrow |1\rangle$ ,  $\gamma'_\phi$  and  $\gamma'$  are the dephasing rate and the energy relaxation rate of the level  $|2\rangle$  of qutrit  $A$  for the decay path  $|2\rangle \rightarrow |0\rangle$ , and  $\gamma''_\phi$  and  $\gamma''$  are the dephasing rate and the energy relaxation rate of the level  $|1\rangle$  of qutrit  $A$  for the decay path  $|1\rangle \rightarrow |0\rangle$ , respectively. The fidelity of the operations is given by

$$\mathcal{F} = \langle \psi_{id} | \tilde{\rho} | \psi_{id} \rangle, \quad (12)$$

where  $|\psi_{id}\rangle$  is the state (8) of the whole system after the above operations, in the ideal case without considering the dissipation of the system during the entire operation; and  $\tilde{\rho}$  is the final density operator of the whole system when the operations are performed in a real situation.

A coherent state  $|\alpha_i\rangle$  can be expressed as  $|\alpha_i\rangle = \exp[-|\alpha_i|^2/2] \sum_{n=0}^{\infty} \frac{\alpha_i^n}{\sqrt{n!}} |n\rangle$  in a Fock-state basis. In our numerical calculation, we consider the first  $m$  terms in the expansions of  $|\alpha_i\rangle$  and  $|-\alpha_i\rangle$ , i.e.,

$$|\alpha_i\rangle \approx \exp[-|\alpha_i|^2/2] \sum_{n=0}^m \frac{\alpha_i^n}{\sqrt{n!}} |n\rangle, \quad (13)$$

$$|-\alpha_i\rangle \approx \exp[-|\alpha_i|^2/2] \sum_{n=0}^m \frac{(-\alpha_i)^n}{\sqrt{n!}} |n\rangle.$$

Under this consideration, the expression of the fidelity above is modified as

$$\mathcal{F} = \frac{\langle \psi_{id} | \tilde{\rho} | \psi_{id} \rangle}{|\langle \psi_{id} | \psi_{id} \rangle|^2}, \quad (14)$$

where  $|\psi_{id}\rangle$  is the state (8) in which the coherence states  $|\alpha_i\rangle$  and  $|-\alpha_i\rangle$  are now replaced by the states given in Eq. (13), and the denominator  $|\langle \psi_{id} | \psi_{id} \rangle|^2$  arises from the normalization of the state  $|\psi_{id}\rangle$ . For simplicity, we consider  $\alpha_1 = \alpha_2 = \alpha_3 = \alpha_4 = \alpha$  in our numerical calculation.

By defining  $\Delta_{c,4} - \Delta_{c,3} = \Delta_{c,3} - \Delta_{c,2} = \Delta_{c,2} - \Delta_{c,1} = s \Delta_{c,1}$ , we have  $\omega_{c,2} = \omega_{c,1} - s \Delta_{c,1}$ ,  $\omega_{c,3} = \omega_{c,1} - 2s \Delta_{c,1}$ , and  $\omega_{c,4} = \omega_{c,1} - 3s \Delta_{c,1}$ . According to  $g_1^2 / \Delta_{c,1} = g_2^2 / \Delta_{c,2} = g_3^2 / \Delta_{c,3} = g_4^2 / \Delta_{c,4}$ , we have  $g_2 = \sqrt{1 + s} g_1$ ,  $g_3 = \sqrt{1 + 2s} g_1$ , and  $g_4 = \sqrt{1 + 3s} g_1$ . For the choice of  $\gamma_\phi^{-1} = (\gamma'_\phi)^{-1} = (\gamma''_\phi)^{-1} = 5 \mu\text{s}$ ,  $\gamma^{-1} = 25 \mu\text{s}$ ,  $(\gamma')^{-1} = 200 \mu\text{s}$ ,  $(\gamma'')^{-1} = 50 \mu\text{s}$ ,  $\kappa_1^{-1} = \kappa_2^{-1} = \kappa_3^{-1} = \kappa_4^{-1} = 20 \mu\text{s}$ ,  $s = 0.5$ , and  $g_1 / 2\pi = 75 \text{ MHz}$ , the fidelity versus the parameter  $\Delta_{c,1} / g_1$  is shown in Fig. 4 where only eight points are plotted and each point is based on the numerical

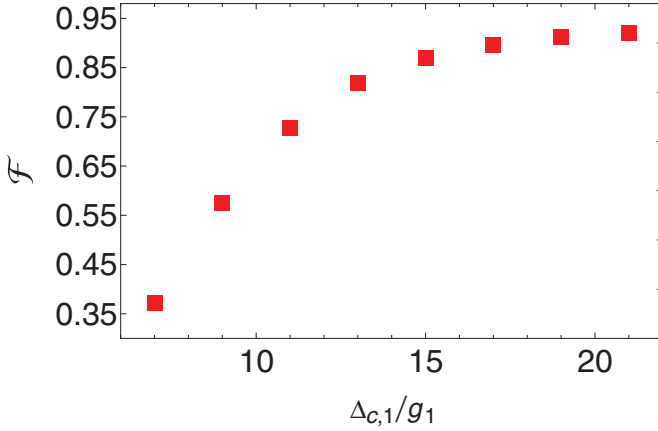


FIG. 4. (Color online) Fidelity versus  $\Delta_{c,1}/g_1$ . The parameters used in the numerical calculation are  $\gamma_\phi^{-1} = (\gamma'_\phi)^{-1} = (\gamma''_\phi)^{-1} = 5 \mu\text{s}$ ,  $\gamma^{-1} = 25 \mu\text{s}$ ,  $(\gamma')^{-1} = 200 \mu\text{s}$ ,  $(\gamma'')^{-1} = 50 \mu\text{s}$ ,  $\kappa_1^{-1} = \kappa_2^{-1} = \kappa_3^{-1} = \kappa_4^{-1} = 20 \mu\text{s}$ ,  $s = 0.5$ , and  $g_1/2\pi = 75 \text{ MHz}$ .

calculation for  $\alpha = 1.1$  and  $m = 3$ . From Fig. 4, it can be seen that a high fidelity  $\sim 93\%$  can be achieved when  $\Delta_{c,1}/g_1 = 20$ . For  $s = 0.5$  here, we have  $g_2/2\pi \sim 92 \text{ MHz}$ ,  $g_3 \sim 106 \text{ MHz}$ , and  $g_4 \sim 119 \text{ MHz}$ . Note that a coupling constant  $\sim 220 \text{ MHz}$  can be reached for a superconducting device coupled to a one-dimensional standing-wave CPW (coplanar waveguide) transmission line resonator [29], and that  $T_1$  and  $T_2$  can be made to be on the order of  $10\text{--}100 \mu\text{s}$  for the state of art superconducting devices at this time [56]. Without loss of generality, assume that the  $|1\rangle \leftrightarrow |2\rangle$  transition frequency of qutrit  $A$  is  $\nu_0 \sim 10 \text{ GHz}$ , and thus the frequencies of cavity 1, 2, 3, and 4 are  $\nu_{c,1} \sim 8.5 \text{ GHz}$ ,  $\nu_{c,2} \sim 7.75 \text{ GHz}$ ,  $\nu_{c,3} \sim 7 \text{ GHz}$ , and  $\nu_{c,4} \sim 6.25 \text{ GHz}$ , respectively [28]. For the cavity frequencies chosen here and for the  $\kappa_1^{-1}, \kappa_2^{-1}, \kappa_3^{-1}, \kappa_4^{-1}$  used in the numerical calculation, the required quality factors for cavities 1, 2, 3, and 4 are  $Q_1 \sim 1.0 \times 10^6$ ,  $Q_2 \sim 9.7 \times 10^5$ ,  $Q_3 \sim 8.8 \times 10^5$ , and  $Q_4 \sim 7.8 \times 10^5$ , respectively. Note that superconducting CPW transmission line resonators with a loaded quality factor  $Q \sim 10^6$  have been experimentally demonstrated [57,58], and planar superconducting resonators with internal quality factors above one million ( $Q > 10^6$ ) have also been reported recently [59]. Our analysis given here demonstrates that preparation of an entangled coherent state of four cavities is possible within the present circuit cavity QED technique.

### C. Discussion

Note that the level  $|1\rangle$  of qutrit  $A$  has longer energy relaxation time and dephasing time than the level  $|2\rangle$ . Thus, we focus on the level  $|2\rangle$  in the following. According to [24], the energy relaxation of the level  $|2\rangle$  of qutrit  $A$  can be enhanced via dressed dephasing of qutrit  $A$  by each resonator. For simplicity, let us consider resonator  $i$ . The effective relaxation rate  $\Gamma_e$  of the level  $|2\rangle$  of qutrit  $A$ , induced due to the dressed dephasing of qutrit  $A$  by the photons of resonator  $i$ , is given by [60]

$$\gamma_e = \gamma \left( 1 - \frac{2\bar{n}_i + 1}{4n_{\text{crit},i}} \right) + \gamma_{k,i} + \gamma_{\Delta,i}\bar{n}_i, \quad (15)$$

where  $\gamma$  is the pure energy relaxation rate of the level  $|2\rangle$  of qutrit  $A$  caused by noise environment,  $\gamma_{k,i}$  is the Purcell decay rate associated with resonator  $i$ ,  $\gamma_{\Delta,i}$  is the measurement and dephasing-induced relaxation rate,  $n_{\text{crit},i} = \Delta_{c,i}^2/4g_i^2$  is the critical photon number for resonator  $i$ , and  $\bar{n}_i$  is the average photon number of resonator  $i$ . One can see from Eq. (15) that to avoid the enhancement of the energy relaxation of the level  $|2\rangle$  (i.e., to obtain  $\gamma_e \leq \gamma$ ), the following condition

$$\bar{n}_i \leq \frac{\gamma - 4n_{\text{crit},i}\gamma_{k,i}}{4n_{\text{crit},i}\gamma_{\Delta,i} - 2\gamma} \quad (16)$$

needs to be satisfied. The result (16) set an upper limit on the average photon number of resonator  $i$  ( $i = 1, 2, 3, 4$ ).

As shown above, a measurement on the states of qutrit  $A$  is needed during preparation of the entangled coherent states of cavities. To the best of our knowledge, all existing proposals for creating entangled coherent states based on cavity QED require a measurement on the states of qubits or qutrits [61].

In the Introduction, we have given a discussion on the significance of entangled coherent states in quantum information processing and communication. Here, we would like to add a few lines regarding the advantages and disadvantages that a network of coherent states might have versus Fock states. The advantages are as follows: when compared with Fock states, (i) coherent states are more easily prepared in experiments, and (ii) they are more robust against decoherence caused by environment and thus can be transmitted over a longer distance. The disadvantage is that both an entangled coherent state and an entangled Fock state may suffer from strong decoherence when the average photon number is large.

## IV. ENTANGLING QUBITS EMBEDDED IN DIFFERENT CAVITIES

In this section, we will show how to prepare a GHZ entangled state of four qubits located at four different cavities. We then give a discussion of the fidelity of the operations. Last, we discuss how to prepare multiple qubits distributed over  $n$  different cavities.

### A. Preparation of GHZ states of four qubits in four cavities

Consider a system composed of four cavities coupled by a superconducting qutrit  $A$  [Fig. 2(b)]. The qutrit  $A$  is initially decoupled from the four cavities [Fig. 5(a)]. Each cavity hosts a two-level qubit 1, 2, 3, or 4, which is represented by a black dot [Fig. 2(b)]. The two levels of each of qubits 1, 2, 3, and 4 are labeled as  $|0\rangle$  (the ground state) and  $|1\rangle$  (the excited state). The qubits (1,2,3,4) are initially decoupled from their respective cavities. Qutrit  $A$  and qubits (1,2,3) are initially prepared in the state  $(|0\rangle + |1\rangle)/\sqrt{2}$ , while qubit 4 is initially in the state  $|0\rangle$ . In addition, each cavity is initially in a vacuum state. The operations for preparing the qubits (1,2,3,4) in a GHZ state are listed in the following steps:

(i) Adjust the level spacings of qubits (1,2,3) to bring the  $|0\rangle \leftrightarrow |1\rangle$  transition of qubit  $i$  resonant with the cavity  $i$  ( $i = 1, 2, 3$ ) for an interaction time  $t_i = \pi/(2g_{r,i})$ , such that the state  $|1\rangle_i |0\rangle_{c,i}$  is transformed to  $-i |0\rangle_i |1\rangle_{c,i}$ , while the state  $|0\rangle_i |0\rangle_{c,i}$  remains unchanged. Here,  $g_{r,i}$  is the resonant coupling constant of qubit  $i$  with cavity  $i$ . After this step, the

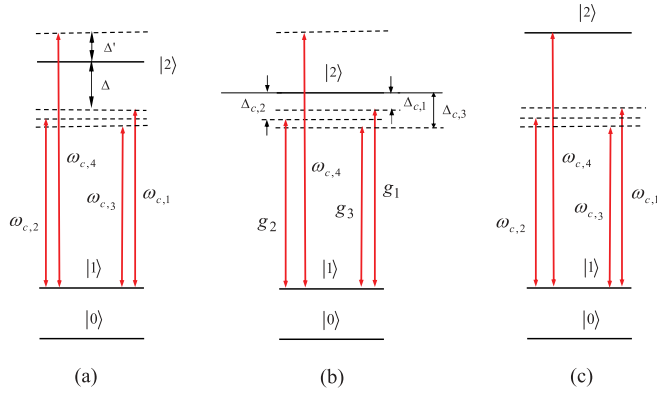


FIG. 5. (Color online) (a) Illustration of qutrit  $A$  decoupled from four cavities or resonators. Here,  $\Delta$  is the large detuning between the  $|1\rangle \leftrightarrow |2\rangle$  transition frequency of qutrit  $A$  and the frequency  $\omega_{c,1}$  of resonator 1, which represents that the  $|1\rangle \leftrightarrow |2\rangle$  transition of qutrit  $A$  is far off resonant with (decoupled from) resonator 1. Since the frequencies  $\omega_{c,1}$ ,  $\omega_{c,2}$ , and  $\omega_{c,3}$  of three resonators 1, 2, and 3 satisfy  $\omega_{c,1} > \omega_{c,2} > \omega_{c,3}$ , the  $|1\rangle \leftrightarrow |2\rangle$  transition of qutrit  $A$  is also far off resonant with (decoupled from) the other three resonators 2, 3, and 4. In addition,  $\Delta'$  is the large detuning between the  $|1\rangle \leftrightarrow |2\rangle$  transition frequency of qutrit  $A$  and the frequency  $\omega_{c,4}$  of resonator 4, which indicates that the  $|1\rangle \leftrightarrow |2\rangle$  transition of qutrit  $A$  is far off resonant with (decoupled from) resonator 4. (b) Illustration of three resonators (1,2,3) each dispersively coupled with the  $|1\rangle \leftrightarrow |2\rangle$  transition of qutrit  $A$ . Here,  $\Delta_{c,i}$  is the large detuning between the  $|1\rangle \leftrightarrow |2\rangle$  transition frequency of qutrit  $A$  and the frequency  $\omega_{c,i}$  of resonator  $i$ , which satisfies  $\Delta_{c,i} \gg g_i$  ( $i = 1, 2, 3$ ). When tuning the level spacings of qutrit  $A$  from Fig. 5(a) to 5(b), the detuning  $\Delta'$  increases, thus qutrit  $A$  remains decoupled from resonator 4. (c) Illustration of resonator 4 resonantly coupled with the  $|1\rangle \leftrightarrow |2\rangle$  transition of qutrit  $A$ . When tuning the level spacings of qutrit  $A$  from Fig. 5(a) to 5(c), the detuning  $\Delta$  increases and thus the  $|1\rangle \leftrightarrow |2\rangle$  transition of qutrit  $A$  remains decoupled from the three cavities 1, 2, and 3.

initial state of the whole system changes to [62]

$$\prod_{i=1}^3 [ |0\rangle_i (|0\rangle_{c,i} - i |1\rangle_{c,i}) ] \otimes |0\rangle_4 |0\rangle_{c,4} (|0\rangle_A + |1\rangle_A). \quad (17)$$

Here and below, a normalization factor is omitted for simplicity.

(ii) Adjust the level spacings of qubits (1,2,3) such that each of these qubits is decoupled from its host cavity, and adjust the level spacings of qutrit  $A$  to bring the  $|1\rangle \leftrightarrow |2\rangle$  transition of this qutrit dispersively coupled to the mode of each of cavities 1, 2, and 3 (i.e.,  $\Delta_{c,i} = \omega_{21} - \omega_{c,i} \gg g_i$  for cavity  $i$  with  $i = 1, 2, 3$ ), while the transition between any other two levels of qutrit  $A$  is far off resonant with (decoupled from) the mode of each of cavities 1, 2, 3 [Fig. 5(b)]. After an interaction time  $t$ , the state (17) changes to

$$\left\{ \prod_{i=1}^3 |0\rangle_i \otimes \left[ \prod_{i=1}^3 (|0\rangle_{c,i} - i |1\rangle_{c,i}) |0\rangle_A + \prod_{i=1}^3 (|0\rangle_{c,i} - i e^{i g_i^2 t / \Delta_{c,i}} |1\rangle_{c,i}) |1\rangle_A \right] \right\} \otimes |0\rangle_4 |0\rangle_{c,4}. \quad (18)$$

With a choice of  $\frac{g_1^2}{\Delta_{c,1}} = \frac{g_2^2}{\Delta_{c,2}} = \frac{g_3^2}{\Delta_{c,3}}$  and for  $g_i^2 \tau / \Delta_{c,i} = \pi$ , we obtain from Eq. (18)

$$\left\{ \prod_{i=1}^3 |0\rangle_i \otimes \left[ \prod_{i=1}^3 (|0\rangle_{c,i} - i |1\rangle_{c,i}) |0\rangle_A + \prod_{i=1}^3 (|0\rangle_{c,i} + i |1\rangle_{c,i}) |1\rangle_A \right] \right\} \otimes |0\rangle_4 |0\rangle_{c,4}. \quad (19)$$

(iii) Adjust the level spacings of qutrit  $A$  to its original configuration [Fig. 5(a)] such that this qutrit is decoupled from each cavity. Then, adjust the level spacings of qubits (1,2,3) to bring the  $|0\rangle \leftrightarrow |1\rangle$  transition of qubit  $i$  ( $i = 1, 2, 3$ ) for an interaction time  $t_i = \pi / (2g_{r,i})$ , such that the state  $|0\rangle_i |1\rangle_{c,i}$  is transformed to  $-i |1\rangle_i |0\rangle_{c,i}$ , while the state  $|0\rangle_i |0\rangle_{c,i}$  remains unchanged. After this step of operation, the state (19) becomes

$$\left[ \prod_{i=1}^3 (|0\rangle_i - |1\rangle_i) |0\rangle_A + \prod_{i=1}^3 (|0\rangle_i + |1\rangle_i) |1\rangle_A \right] \otimes |0\rangle_4 \prod_{i=1}^4 |0\rangle_{c,i}. \quad (20)$$

The result (20) shows that after this step, the qubit-qutrit system is disentangled from the cavities but the qubits (1,2,3) are entangled with qutrit  $A$ .

(iv) Adjust the level spacings of the qubits (1,2,3) such that these qubits are decoupled from their cavities. Then, adjust the level spacings of qutrit  $A$  such that the  $|1\rangle \leftrightarrow |2\rangle$  transition of qutrit  $A$  is resonant with the mode of cavity 4 [Fig. 5(c)]. After an interaction time  $t_A = \pi / (2g_{r,A})$ , the state  $|1\rangle_A |0\rangle_{c,4}$  is transformed to  $-i |0\rangle_A |1\rangle_{c,4}$ , while the state  $|0\rangle_A |0\rangle_{c,4}$  remains unchanged. Here and below,  $g_{r,A}$  is the resonant coupling constant of qutrit  $A$  with cavity 4, while  $g_{r,4}$  is the resonant coupling constant of qubit 4 with cavity 4. After this step, the state (20) changes to

$$\left[ \prod_{i=1}^3 (|0\rangle_i - |1\rangle_i) |0\rangle_{c,4} - i \prod_{i=1}^3 (|0\rangle_i + |1\rangle_i) |1\rangle_{c,4} \right] \otimes |0\rangle_A |0\rangle_4 \prod_{i=1}^3 |0\rangle_{c,i}. \quad (21)$$

(v) Adjust the level spacings of the qubit 4 such that this qubit is now resonant with the mode of cavity 4 for an interaction time  $t_4 = \pi / (2g_{r,4})$  to transform the state  $|0\rangle_4 |1\rangle_{c,4}$  to  $-i |1\rangle_4 |0\rangle_{c,4}$ , while the state  $|0\rangle_4 |0\rangle_{c,4}$  remains unchanged. As a result, the state (21) becomes

$$\left[ \prod_{i=1}^3 (|0\rangle_i - |1\rangle_i) |0\rangle_4 - \prod_{i=1}^3 (|0\rangle_i + |1\rangle_i) |1\rangle_4 \right] \otimes |0\rangle_A \prod_{i=1}^3 |0\rangle_{c,i}, \quad (22)$$

where  $|-\rangle_i = |0\rangle_i - |1\rangle_i$  and  $|+\rangle_i = |0\rangle_i + |1\rangle_i$ . Note that after this step, the level spacings of

qubit 4 need adjusted to have qubit 4 to be decoupled from cavity 4.

From Eq. (22), one can see that after the above operations, the qubits (1,2,3,4) are prepared in a GHZ state while each cavity returns to its original vacuum state.

We should mention that because the level spacing between the two levels  $|1\rangle$  and  $|2\rangle$  of qutrit  $A$  in Fig. 5(a) is set to be greater than that in Fig. 5(b), qutrit  $A$  remains off resonant with any of the three resonators 1, 2, and 3 during tuning the level structure of qutrit  $A$  from Fig. 5(a) to 5(b). Also, when tuning the level spacings of qutrit  $A$  from Fig. 5(a) to 5(b), the detuning between the  $|1\rangle \leftrightarrow |2\rangle$  transition frequency of qutrit  $A$  and the frequency of resonator 4 increases, and thus qutrit  $A$  is decoupled from resonator 4 during the operations of steps (i)–(iv) above.

During the above GHZ-state preparation for the four qubits (1,2,3,4), the other qubits in each cavity, which are represented by the gray dots in Fig. 2(b), are decoupled from the cavity mode by prior adjustment of their level spacings.

### B. Fidelity

Let us now study the fidelity of the entanglement preparation above. We note that since the resonant interactions are used in steps (i), (iii), (iv) and (v), these steps can be completed within a very short time (e.g., by increasing the resonant device-cavity coupling constants), such that decoherence of the qubits, the qutrit  $A$ , and the cavities is negligibly small. In this case, decoherence of the system would have a negative impact on the step (ii) of the operation due to the use of the qutrit-cavity dispersive interaction.

By defining  $\Delta_{c,3} - \Delta_{c,2} = \Delta_{c,2} - \Delta_{c,1} = s\Delta_{c,1}$ , we have  $\omega_{c,2} = \omega_{c,1} - s\Delta_{c,1}$  and  $\omega_{c,3} = \omega_{c,1} - 2s\Delta_{c,1}$ . In addition, according to  $g_1^2/\Delta_{c,1} = g_2^2/\Delta_{c,2} = g_3^2/\Delta_{c,3}$ , we have  $g_2 = \sqrt{1+s}g_1$  and  $g_3 = \sqrt{1+2s}g_1$ . For the choice of  $\gamma_\varphi^{-1} = (\gamma'_\varphi)^{-1} = (\gamma''_\varphi)^{-1} = 5 \mu\text{s}$ ,  $\gamma^{-1} = 25 \mu\text{s}$ ,  $(\gamma')^{-1} = 200\mu\text{s}$ ,  $(\gamma'')^{-1} = 50 \mu\text{s}$ ,  $\kappa_1^{-1} = \kappa_2^{-1} = \kappa_3^{-1} = 20 \mu\text{s}$ ,  $\Delta_{c,1} = 10g_1$ , and  $g_1/2\pi = 100 \text{ MHz}$ , the fidelity versus the parameter  $s$  is shown in Fig. 6, from which one can see that a high fidelity  $\sim 96\%$  can be achieved when  $s = 1$ , which corresponds to

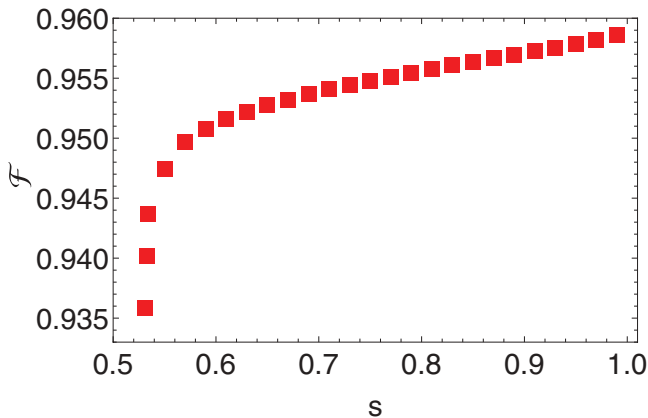


FIG. 6. (Color online) Fidelity versus  $s$ . The parameters used in the numerical calculation are  $\gamma_\varphi^{-1} = (\gamma'_\varphi)^{-1} = (\gamma''_\varphi)^{-1} = 5 \mu\text{s}$ ,  $\gamma^{-1} = 25 \mu\text{s}$ ,  $(\gamma')^{-1} = 200 \mu\text{s}$ ,  $(\gamma'')^{-1} = 50 \mu\text{s}$ ,  $\kappa_1^{-1} = \kappa_2^{-1} = \kappa_3^{-1} = 20 \mu\text{s}$ ,  $\Delta_{c,1} = 10g_1$ , and  $g_1/2\pi = 100 \text{ MHz}$ .

the case of  $g_2/2\pi \sim 141 \text{ MHz}$  and  $g_3 \sim 173 \text{ MHz}$ . In the following, we consider the case of  $s = 1$ . Without loss of generality, assume that the  $|1\rangle \leftrightarrow |2\rangle$  transition frequency of qutrit  $A$  is  $\nu_0 \sim 8.5 \text{ GHz}$ , and thus the frequency of cavity 1, the frequency of cavity 2, and the frequency of cavity 3 are  $\nu_{c,1} \sim 7.5 \text{ GHz}$ ,  $\nu_{c,2} \sim 6.5 \text{ GHz}$ , and  $\nu_{c,3} \sim 5.5 \text{ GHz}$ , respectively. For the cavity frequencies chosen here and for the  $\kappa_1^{-1}, \kappa_2^{-1}, \kappa_3^{-1}$  used in our numerical calculation, the required quality factors for cavities 1, 2, and 3 are  $Q_1 \sim 9.4 \times 10^5$ ,  $Q_2 \sim 8.2 \times 10^5$ , and  $Q_3 \sim 6.9 \times 10^5$ , respectively. Finally, it is noted that since only resonant interaction of qutrit  $A$  with cavity 4 is involved during the above operations, the requirement for cavity 4 is greatly reduced when compared with cavities 1, 2, and 3. Our analysis given here shows that preparation of a GHZ entangled state of four qubits located at four cavities is possible within the present circuit cavity QED technique.

### C. Preparation of GHZ states of multiple qubits embedded in $n$ cavities

One can easily verify that, in principle, by using a superconducting qutrit coupled to  $n$  cavities,  $n$  qubits (1,2, ...,  $n$ ) initially in the state  $\prod_{i=1}^{n-1} |+\rangle_i \otimes |0\rangle_n$ , which are respectively located in the different  $n$  cavities, can be prepared in an entangled GHZ state  $\prod_{i=1}^{n-1} |-\rangle_i |0\rangle_n - \prod_{i=1}^n |+\rangle_i |1\rangle_n$  by using the same procedure described above.

Furthermore, based on the prepared GHZ state of  $n$  qubits (1,2, ...,  $n$ ), all other qubits (not entangled initially) in the cavities can be entangled with the GHZ-state qubits (1,2, ...,  $n$ ), through intracavity controlled-NOT (CNOT) operations on the qubits in each cavity by using the GHZ-state qubit in each cavity (i.e., qubit 1, 2, ..., or  $n$ ) as the control while the other qubits as the targets. To see this clearly, let us consider Fig. 2(b), where the three qubits in cavity  $i$  ( $i = 1,2,3,4$ ) are the black-dot qubit  $i$  and the two gray-dot qubits, labeled as qubits  $i2$  and  $i3$  here. Suppose that the four black-dot qubits (1,2,3,4) (i.e., the GHZ-state qubits) were prepared in the GHZ state of Eq. (17), and each gray-dot qubit is initially in the state  $|+\rangle$ . By performing CNOT on various qubit pairs in each cavity, i.e.,  $C_{i,i2}$  and  $C_{i,i3}$  on the qubit pairs  $(i,i2)$  and  $(i,i3)$  for cavity  $i$ , one can have all qubits in the four cavities (both black-dot and gray-dot qubits) prepared in a GHZ state  $\prod_{i=1}^4 |-\rangle_i |-\rangle_{i2} |-\rangle_{i3} - \prod_{i=1}^4 |+\rangle_i |+\rangle_{i2} |+\rangle_{i3}$ . Here,  $C_{i,i2}$ , defined in the basis  $\{|+\rangle_i |+\rangle_{i2}, |-\rangle_i |+\rangle_{i2}, |+\rangle_i |-\rangle_{i2}, |-\rangle_i |-\rangle_{i2}\}$  represents a CNOT with qubit  $i$  (the GHZ-state qubit) as the control with qubit  $i2$  as the target, which results in the transformation  $|-\rangle_i |+\rangle_{i2} \rightarrow |-\rangle_i |-\rangle_{i2}$ , while it leaves the state  $|+\rangle_i |+\rangle_{i2}$  unchanged. A similar definition applies to  $C_{i,i3}$ . Alternatively, using the prepared GHZ state of  $n$  qubits (1,2, ...,  $n$ ), one can have all other qubits in the cavities to be entangled with the GHZ-state qubits (1,2, ...,  $n$ ) by performing an intracavity multiqubit CNOT with the GHZ-state qubit (control qubit) simultaneously controlling all other qubits (target qubits) in each cavity [26].

Experimentally, it has been demonstrated successfully on circuits consisting up to 128 flux qubits that crosstalk from control circuitry can be essentially eliminated and/or

corrected by practicing proper circuit designs and developing corresponding multilayer fabrication processes [63]. Hence, frequency crowding for multiple qubits in one resonator and control of large numbers of qubits do not present a fundamental and/or practical problem for the proposed protocol.

### V. POSSIBILITY OF A TWO-DIMENSIONAL QUANTUM NETWORK

The four resonators coupled by a coupler superconducting qutrit may be used as a basic circuit block to build a two-dimensional (2D) quantum network for quantum information processing, as depicted in Fig. 7. In this network, for any two of qubits and qutrits coupled or connected by a resonator (e.g., qubit  $a$  and qutrit  $A$ , qutrits  $A$  and  $B$ , and so on), quantum operations can be performed on them directly because they can interact with each other, mediated by their shared resonator. In addition, for any two qubits located at different cavities or resonators, quantum operations can be performed through information transfer. To see this, let us consider two distant qubits  $a$  and  $b$  in the network (Fig. 7). To perform a quantum operation on the two qubits  $a$  and  $b$ , one can do the following. First, (i) transfer the quantum information stored in qubit  $a$  to the coupler qutrit  $D$  via a transfer sequence  $a \rightarrow A \rightarrow B \rightarrow C \rightarrow D$ , (ii) perform the quantum operation on the coupler qutrit  $D$  and qubit  $b$ , and then (iii) transfer the quantum information of the coupler qutrit  $D$  back to qubit  $a$  through a transfer sequence  $D \rightarrow C \rightarrow B \rightarrow A \rightarrow a$ . In this way, the quantum operation is performed on the two distant qubits  $a$  and  $b$  indirectly. It should be mentioned that to perform a quantum operation on two qubits at different cavities, the intermediate coupler qutrits (e.g., qutrits  $A$ ,  $B$ , and  $C$  for the example given here) need to be initially prepared in the ground state  $|0\rangle$  as required by quantum information transfer [e.g., this can be seen from the state transformation  $(\alpha|0\rangle_a + \beta|1\rangle_a)|0\rangle_A \rightarrow$

$|0\rangle_a(\alpha|0\rangle_A + \beta|1\rangle_A)$  for the information transfer from qubit  $a$  to the coupler qutrit  $A$ ).

An architecture for quantum computing based on superconducting circuits, where on-chip planar microwave resonators are arranged in a two-dimensional grid with a qubit sitting at each intersection, was previously proposed [64]. However, our present proposal is different from that in the following. For the architecture in Ref. [64], each qubit at an intersection is coupled to two cavity modes, i.e., one cavity mode belongs to a horizontal cavity built on the top layer, while the other cavity mode belongs to a vertical cavity built at a second layer at the bottom. In contrast, in our case, as shown in Fig. 7, all resonators and coupler qutrits are arranged in the same plane, which is relatively easy to implement in experiments.

Finally, Ref. [65] analyzes the performance of the resonator plus zero-qubit (REZQU) architecture in which the qubits are complemented with memory resonators and coupled via a resonator bus. We note that in Ref. [65], the memory resonators are coupled via a common resonator bus, while in our proposal the cavities are coupled via a coupler qutrit. Hence, our architecture is quite different from that in [65].

We remark that many details on possible scalability of the protocol (including quantum error correction) need to be addressed. However, this requires a lengthy and complex analysis, which is beyond the scope of this work. We would like to leave them as open questions to be addressed in future work.

### VI. CONCLUSION

We have proposed a method for creating four-resonator entangled coherent states and preparing a GHZ state of four qubits in four cavities by using a superconducting qutrit as the coupler. In principle, this proposal can be extended to create entangled coherent states of  $n$  resonators and to prepare GHZ states of  $n$  qubits distributed over  $n$  cavities in a network, with the same operational steps and the operation time as those of the four-resonator case described above. This proposal is quite general and can be applied to the case when the coupler qutrit is a different physical system with three levels, such as a quantum dot or a NV center. Finally, it is noted that the structure of four resonators coupled by a coupler qutrit can be used as a basic circuit block to build a two-dimensional quantum network, which may be useful for scalable quantum information processing.

### ACKNOWLEDGMENTS

S. Han was supported in part by DMEA. C. P. Yang was supported in part by the National Natural Science Foundation of China under Grant No. 11074062, the Zhejiang Natural Science Foundation under Grant No. Y6100098, the Open Fund from the SKLPS of ECNU, and the funds from Hangzhou Normal University. Q. P. Su was supported by the National Natural Science Foundation of China under Grant No. 11147186. S. B. Zheng was supported by the Major State Basic Research Development Program of China under Grant No. 2012CB921601.

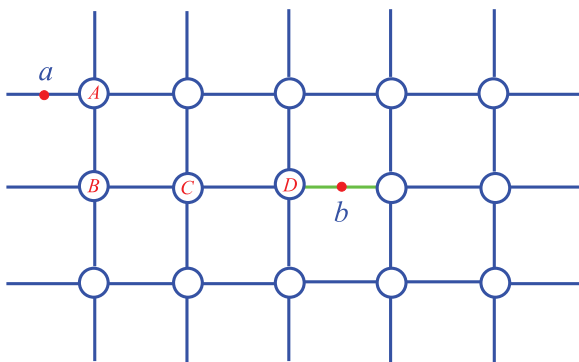


FIG. 7. (Color online) Two-dimensional linear network of resonators, qubits, and qutrits. A short line represents a resonator and each circle represents a coupler qutrit. The two red dots represent qubits  $a$  and  $b$ . The coupler qutrits  $A$ ,  $B$ , and  $C$  are used to transfer information stored in qubit  $a$  to the coupler qutrit  $D$ . They are also used to transfer information of the coupler qutrit  $D$  back to qubit  $a$  after a quantum operation is performed on the coupler qutrit  $D$  and qubit  $b$ , which interact with each other through a resonator (i.e., the green short line).



- [1] J. Q. You and F. Nori, *Nature (London)* **474**, 589 (2011).
- [2] J. Clarke and F. K. Wilhelm, *Nature (London)* **453**, 1031 (2008).
- [3] S. Filipp *et al.*, *Phys. Rev. Lett.* **102**, 200402 (2009).
- [4] R. C. Bialczak *et al.*, *Nat. Phys.* **6**, 409 (2010).
- [5] M. Neeley *et al.*, *Nature (London)* **467**, 570 (2010).
- [6] T. Yamamoto *et al.*, *Phys. Rev. B* **82**, 184515 (2010).
- [7] M. D. Reed, L. DiCarlo, B. R. Johnson, L. Sun, D. I. Schuster, L. Frunzio, and R. J. Schoelkopf, *Phys. Rev. Lett.* **105**, 173601 (2010).
- [8] C. P. Yang, Shih-I. Chu, and S. Han, *Phys. Rev. A* **67**, 042311 (2003).
- [9] J. Majer *et al.*, *Nature (London)* **449**, 443 (2007).
- [10] L. DiCarlo *et al.*, *Nature (London)* **460**, 240 (2009).
- [11] A. Blais, R. S. Huang, A. Wallraff, S. M. Girvin, and R. J. Schoelkopf, *Phys. Rev. A* **69**, 062320 (2004).
- [12] C. P. Yang, Shih-I. Chu, and S. Han, *Phys. Rev. Lett.* **92**, 117902 (2004).
- [13] A. Wallraff *et al.*, *Nature (London)* **431**, 162 (2004).
- [14] I. Chiorescu *et al.*, *Nature (London)* **431**, 159 (2004).
- [15] F. Marquardt and C. Bruder, *Phys. Rev. B* **63**, 054514 (2001).
- [16] Y. X. Liu, L. F. Wei, and F. Nori, *Europhys. Lett.* **67**, 941 (2004).
- [17] K. Moon and S. M. Girvin, *Phys. Rev. Lett.* **95**, 140504 (2005).
- [18] F. Marquardt, *Phys. Rev. B* **76**, 205416 (2007); M. Mariani *et al.*, [arXiv:cond-mat/0509737](https://arxiv.org/abs/cond-mat/0509737).
- [19] M. Hofheinz *et al.*, *Nature (London)* **454**, 310 (2008); H. Wang *et al.*, *Phys. Rev. Lett.* **101**, 240401 (2008).
- [20] M. Hofheinz *et al.*, *Nature (London)* **459**, 546 (2009).
- [21] F. Plastina and G. Falci, *Phys. Rev. B* **67**, 224514 (2003).
- [22] A. Blais, A. Maassen van den Brink, and A. M. Zagoskin, *Phys. Rev. Lett.* **90**, 127901 (2003).
- [23] J. Q. You and F. Nori, *Phys. Rev. B* **68**, 064509 (2003).
- [24] F. Helmer and F. Marquardt, *Phys. Rev. A* **79**, 052328 (2009).
- [25] L. S. Bishop *et al.*, *New J. Phys.* **11**, 073040 (2009).
- [26] C. P. Yang, Y. X. Liu, and F. Nori, *Phys. Rev. A* **81**, 062323 (2010).
- [27] C. P. Yang, S. B. Zheng, and F. Nori, *Phys. Rev. A* **82**, 062326 (2010).
- [28] P. J. Leek, S. Filipp, P. Maurer, M. Baur, R. Bianchetti, J. M. Fink, M. Goppl, L. Steffen, and A. Wallraff, *Phys. Rev. B* **79**, 180511(R) (2009).
- [29] L. DiCarlo *et al.*, *Nature (London)* **467**, 574 (2010).
- [30] M. Mariani *et al.*, *Science* **334**, 61 (2011).
- [31] A. Fedorov, L. Steffen, M. Baur, M. P. da Silva, and A. Wallraff, *Nature (London)* **481**, 170 (2012).
- [32] M. Mariani, F. Deppe, A. Marx, R. Gross, F. K. Wilhelm, and E. Solano, *Phys. Rev. B* **78**, 104508 (2008).
- [33] F. W. Strauch, K. Jacobs, and R. W. Simmonds, *Phys. Rev. Lett.* **105**, 050501 (2010).
- [34] H. Wang *et al.*, *Phys. Rev. Lett.* **106**, 060401 (2011).
- [35] M. Mariani *et al.*, *Nat. Phys.* **7**, 287 (2011).
- [36] M. Brune, E. Hagley, J. Dreyer, X. Maitre, A. Maali, C. Wunderlich, J. M. Raimond, and S. Haroche, *Phys. Rev. Lett.* **77**, 4887 (1996).
- [37] H. Jeong and M. S. Kim, *Phys. Rev. A* **65**, 042305 (2002).
- [38] T. C. Ralph, A. Gilchrist, G. J. Milburn, W. J. Munro, and S. Glancy, *Phys. Rev. A* **68**, 042319 (2003).
- [39] N. B. An, *Phys. Rev. A* **68**, 022321 (2003).
- [40] P. vanLoock, N. Lutkenhaus, W. J. Munro, and K. Nemoto, *Phys. Rev. A* **78**, 062319 (2008).
- [41] F. Grosshans and P. Grangier, *Phys. Rev. Lett.* **88**, 057902 (2002).
- [42] B. Kraus and J. I. Cirac, *Phys. Rev. Lett.* **92**, 013602 (2004).
- [43] J. Lee, M. Paternostro, M. S. Kim, and S. Bose, *Phys. Rev. Lett.* **96**, 080501 (2006).
- [44] A. Gilchrist, P. Deuar, and M. D. Reid, *Phys. Rev. Lett.* **80**, 3169 (1998); *Phys. Rev. A* **60**, 4259 (1999).
- [45] M. Hillery, V. Buzek, and A. Berthiaume, *Phys. Rev. A* **59**, 1829 (1999).
- [46] See, for many references, S. Bose, V. Vedral, and P. L. Knight, *Phys. Rev. A* **57**, 822 (1998).
- [47] G. C. Guo and S. B. Zheng, *Phys. Lett. A* **223**, 332 (1996); M. J. Holland, D. F. Walls, and P. Zoller, *Phys. Rev. Lett.* **67**, 1716 (1991).
- [48] Y. X. Liu, J. Q. You, L. F. Wei, C. P. Sun, and F. Nori, *Phys. Rev. Lett.* **95**, 087001 (2005).
- [49] S. Han, J. Lapointe, and J. E. Lukens, *Single-Electron Tunneling and Mesoscopic Devices* (Springer, Berlin, 1991), Vol. 31, pp. 219–222.
- [50] M. Neeley *et al.*, *Nat. Phys.* **4**, 523 (2008).
- [51] C. P. Yang, *Phys. Rev. A* **82**, 054303 (2010).
- [52] J. Q. You and F. Nori, *Phys. Today* **58**(11), 42 (2005).
- [53] A. Palacios-Laloy, F. Nguyen, F. Mallet, P. Bertet, D. Vion, and D. Esteve, *J. Low Temp. Phys.* **151**, 1034 (2008).
- [54] R. Harris *et al.*, *Phys. Rev. Lett.* **98**, 177001 (2007).
- [55] S. J. Srinivasan, A. J. Hoffman, J. M. Gambetta, and A. A. Houck, *Phys. Rev. Lett.* **106**, 083601 (2011).
- [56] J. Bylander *et al.*, *Nat. Phys.* **7**, 565 (2011); H. Paik *et al.*, *Phys. Rev. Lett.* **107**, 240501 (2011); J. M. Chow *et al.*, *ibid.* **109**, 060501 (2012); C. Rigetti *et al.*, *Phys. Rev. B* **86**, 100506(R) (2012).
- [57] W. Chen, D. A. Bennett, V. Patel, and J. E. Lukens, *Supercond. Sci. Technol.* **21**, 075013 (2008).
- [58] P. J. Leek, M. Baur, J. M. Fink, R. Bianchetti, L. Steffen, S. Filipp, and A. Wallraff, *Phys. Rev. Lett.* **104**, 100504 (2010).
- [59] A. Megrant *et al.*, *Appl. Phys. Lett.* **100**, 113510 (2012).
- [60] M. Boissonneault, J. M. Gambetta, and A. Blais, *Phys. Rev. A* **77**, 060305(R) (2008).
- [61] E. Solano, G. S. Agarwal, and H. Walther, *Phys. Rev. Lett.* **90**, 027903 (2003); C. C. Gerry, *Phys. Rev. A* **54**, R2529 (1996); G. C. Guo and S. B. Zheng, *Opt. Commun.* **133**, 142 (1997); S. B. Zheng, *Quantum Semiclass. Opt.* **10**, 691 (1998); C. P. Yang and G. C. Guo, *J. Phys. B: At., Mol. Opt. Phys.* **32**, 3309 (1999); J. H. Guo, *Commun. Theor. Phys.* **41**, 37 (2004); X. B. Zou and W. Mathis, *Phys. Lett. A* **337**, 305 (2005); M. Y. Chen and W. M. Zhang, *AIP Conf. Proc.* **1074**, 38 (2008).
- [62] C. P. Yang and S. Han, *Phys. Rev. A* **73**, 032317 (2006).
- [63] R. Harris *et al.*, *Phys. Rev. B* **81**, 134510 (2010); **82**, 024511 (2010); M. W. Johnson *et al.*, *Nature (London)* **473**, 194 (2011).
- [64] F. Helmer, M. Mariani, A. G. Fowler, J. V. Delft, E. Solano, and F. Marquardt, *Europhys. Lett.* **85**, 50007 (2009).
- [65] A. Galiatdinov, A. N. Korotkov, and J. M. Martinis, [arXiv:1105.3997](https://arxiv.org/abs/1105.3997).